Molecular Crystals and Liquid Crystals
Publication details, including instructions for authors and subscription information:
http://www.tandfonline.com/loi/gmcl20

Accelerating the Cholesteric Helix Restoring by a Dual Frequency Compound

Karen Allahverdyan [a b] & Tigran Galstian [a]

[a] Center for Optics, Photonics and Laser, Department of Physics, Engineering Physics and Optics, Laval University, Pav. d'Optique-Photonique, 2375 Rue de la Terrasse, Québec, G1V 0A6, Canada

[b] Department of Physics, Yerevan State University, 1 Alex Manoogian, 0025 Yerevan, Armenia

Version of record first published: 15 May 2012.

To cite this article: Karen Allahverdyan & Tigran Galstian (2012): Accelerating the Cholesteric Helix Restoring by a Dual Frequency Compound, Molecular Crystals and Liquid Crystals, 560:1, 35-48

To link to this article: http://dx.doi.org/10.1080/15421406.2012.661960

Mol. Cryst. Liq. Cryst., Vol. 560: pp. 35–48, 2012

ISSN: 1542-1406 print/1563-5287 online
DOI: 10.1080/15421406.2012.661960

Taylor & Francis
Taylor & Francis Group

Accelerating the Cholesteric Helix Restoring by a Dual Frequency Compound

KAREN ALLAHVERDYAN[1,2] AND TIGRAN GALSTIAN[1,*]

[1]Center for Optics, Photonics and Laser, Department of Physics, Engineering Physics and Optics, Laval University, Pav. d'Optique-Photonique, 2375 Rue de la Terrasse, Québec, G1V 0A6, Canada
[2]Department of Physics, Yerevan State University, 1 Alex Manoogian, 0025 Yerevan, Armenia

We report the creation and the use of dual frequency cholesteric liquid crystal mixtures for the dynamic electrical unwinding and forced (accelerated) restoring of their molecular helix. The use of a cholesteric in a mixture with a dual frequency nematic shifts the resonant wavelength to the near infrared area. We use polarimetric transmission measurements (out of resonance) to check the effective birefringence of the cell as well as the resonant reflection (at near infra red) to characterize the dynamics of unwinding and restoring processes. The restoring process is accelerated almost by an order of magnitude for quite moderate voltages used.

Keywords Cholesteric liquid crystals; dual frequency liquid crystal; electrooptic switch; frequency control; liquid crystals; polarimetry; resonant reflection

Introduction

Liquid crystal (LC) materials have been successfully used in various light modulation applications, [1,2]. However, the inherent anisotropy operation of majority of LCs requires the use of polarizers, which reduces light transmission (increasing thus the power consumption), increases the cost of those modulators and reduces their long term stability.

One of alternative (polarization-free) avenues, explored so far, was the use of cholesteric LCs (CLCs), which naturally form periodic helicoidal molecular structures reflecting light in a specific "resonant" wavelength band and having a circular polarization that is replicating the helix of the CLC, [3,4]. Several mechanisms have been explored so far to control the reflection properties of those materials (position of the bandgap, its strength and bandwidth, etc. (see, e.g., Ref. [5–13]). While the obtained results are very encouraging, there are however several drawbacks with the use of CLCs too. First, the above-mentioned reflection band is relatively narrow (at the order of 50 nm) for broad band applications, such as solar filters or camera shutters. Second, the reflection of natural light (originating from a lamp, LED, sun, etc.) is only 50% since the resonant reflection happens only for the appropriate circular polarization, [3]. Finally, the demonstrated so far dynamic modulations of the

*Address correspondence to Tigran Galstian, Center for Optics, Photonics and Laser, Department of Physics, Engineering Physics and Optics, Laval University, Pav. d'Optique-Photonique, 2375 Rue de la Terrasse, Québec, G1V 0A6, Canada. Phone: 1-418-6562025. E-mail: galstian@phy.ulaval.ca

resonant reflection of CLCs (spectral shift, unwinding, etc.) are relatively slow to recover (sub-millisecond switching times would be needed for imaging or color TV applications). Significant efforts have been deployed to broaden the resonant reflection band and to increase the reflection coefficient [14–16], see also [17,18] and references therein. To the best of our knowledge, the possibilities to accelerate the helix restoring were not explored as intensively as the two above mentioned directions. There are several reports of using CLCs with dual frequency functionality in light shutters (with photo curable materials), thin photonic bangap structures, etc. [19–24]. However, we were not able to find the details of material preparation and dynamic transition characterizations.

In the present work, we were particularly interested by the electrical unwinding of the helix of the CLC CB15 (from Merck). We have thus focused our efforts on the problem of slow restoring of the CLC helix in view of exploring the possible ways of its acceleration. The approach we have used here was based on a mixture of two LC materials, in a way, to preserve the helical structure, while creating two frequency zones (for the electrical driving signals) for which the developed mixture has respectively positive and negative dielectric anisotropy (enabling thus the so called "dual-frquency" operation) allowing the fast "forced" recovery. Thus, we present below the preliminar results of the studies of the material composition developed as well as the electro-optical and morphological properties of cells containing this compound.

Materials Used

The material composition used was obtained by mixing two LCs: the CLC, called CB15, and the nematic LC, called MLC 2048, (both from Merck). Those materials were mixed in two concentrations to obtain two mixtures, the first one containing 33 wt% of CB15 and 67 wt% of MLC 2048 (further referred as Mix 33) and the second one contained 41 wt% of CB15 and 59 wt% of MLC 2048 (further referred as Mix 41). The choice of those compounds was based on the desired dielectric parameters (see later) as well as the material availability. The CB15 is a right handed CLC with a resonant band gap in the green region of light spectra (∼520 nm–560 nm) at room temperature. Unfortunately, Merck was not able to provide more data concerning the dielectric and optical parameters of the CB15. We have however recently measured and reported (Ref. [13]) some of its optical parameters at room temperature (see also Ref. [25]). Most importantly, it was shown that the dielectric anisotropy of the CB15 at low frequencies (1 kHz) is negative.

To prepare the current mixtures, we have proceeded to very approximate (qualitative) measurements of corresponding dielectric constants of each material component as well as of the final mixture. Thus, planar aligned commercial cells (L = 50 μm thick) were fabricated (and filled with our materials) and subjected to capacitance measurements ("HP 4192" Impedance Analyser was used) at different environmental temperatures. Figure 1 shows the driving electrical frequency dependence of measured dielectric constants. First we have measured (with very weak electrical excitation to avoid reorientation effects) the capacitance of the cell and thus the dielectric constants of materials at room temperature (20°C, squares) in their liquid crystalline phase. We attribute the obtained values to the "ordinary" dielectric constant $\varepsilon_\perp$ thanks to the good planar alignment of the cell. Then we heat the cell to achieve the isotropic phase (60°C, triangles) of the material and measure it again to obtain (approximately) the average dielectric constant ε_{av}. Finally we calculate the parallel dielectric constant $\varepsilon_\parallel$ by the formula $\varepsilon_{av} \approx (\varepsilon_\parallel + 2\,\varepsilon_\perp)/2$. We must emphasize

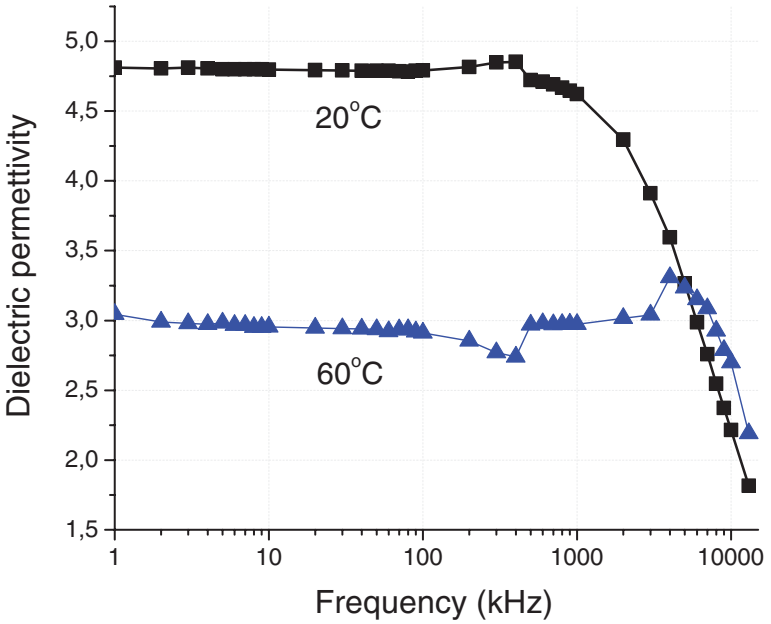

Figure 1. Qualitative dependence of CB15's dielectric permittivity upon the electric field frequency in the CLC (20°C) and isotropy (60°C) phases.

again that those data must be considered as very qualitative. The main goal here was the rough identification of approximate concentrations that would allow us to obtain a "dual frequency" helicoidal mixture. To show the degree of imprecision of our estimations, we have used the same technique to do similar measurements also on the second component of our mixture (the MLC 2048), which is much better known and described in the literature, Fig. 2. Its nematic-isotropic phase transition temperature is 106°C, the ordinary refractive index and anisotropy at 20°C are respectively $n_o = 1.4978$ and $\Delta n = 0.2214$ (both measured at 589 nm), [26]. This is a "dual frequency" nematic LC that was largely used to accelerate the "back" reorientation, e.g. in LC scatterers or retarders [27,28]. Indeed, the dielectric anisotropy of this LC is positive for "low" frequencies (<10 kHz at 20°C) and is negative for "high" frequencies (>50 kHz at 20°C), see Fig. 2(a) ([29]). The simple set-up and method we have used (to measure the dielectric constants of our materials) provide rather similar values (compared to those reported elsewhere) when applied to the MLC 2048, Fig. 2.

The final mixtures (Mix 33 and Mix 41) were thus made, taking into account the above mentioned measurements to possess low-frequency positive dielectric anisotropy (to enable the electrical unwinding of the helix) and high frequency negative dielectric anisotropy (for forced restoring of the helix, see later).

Cell Fabrication and Characterization

The experimental cells were fabricated and filled by standard capillarity method (filled at 20°C). First of all, the indium tin oxide (ITO) coated substrates (commercially procured) were washed in the ultrasonic bath (for 8–10 minutes, in soap-water solution, 8–10 min.

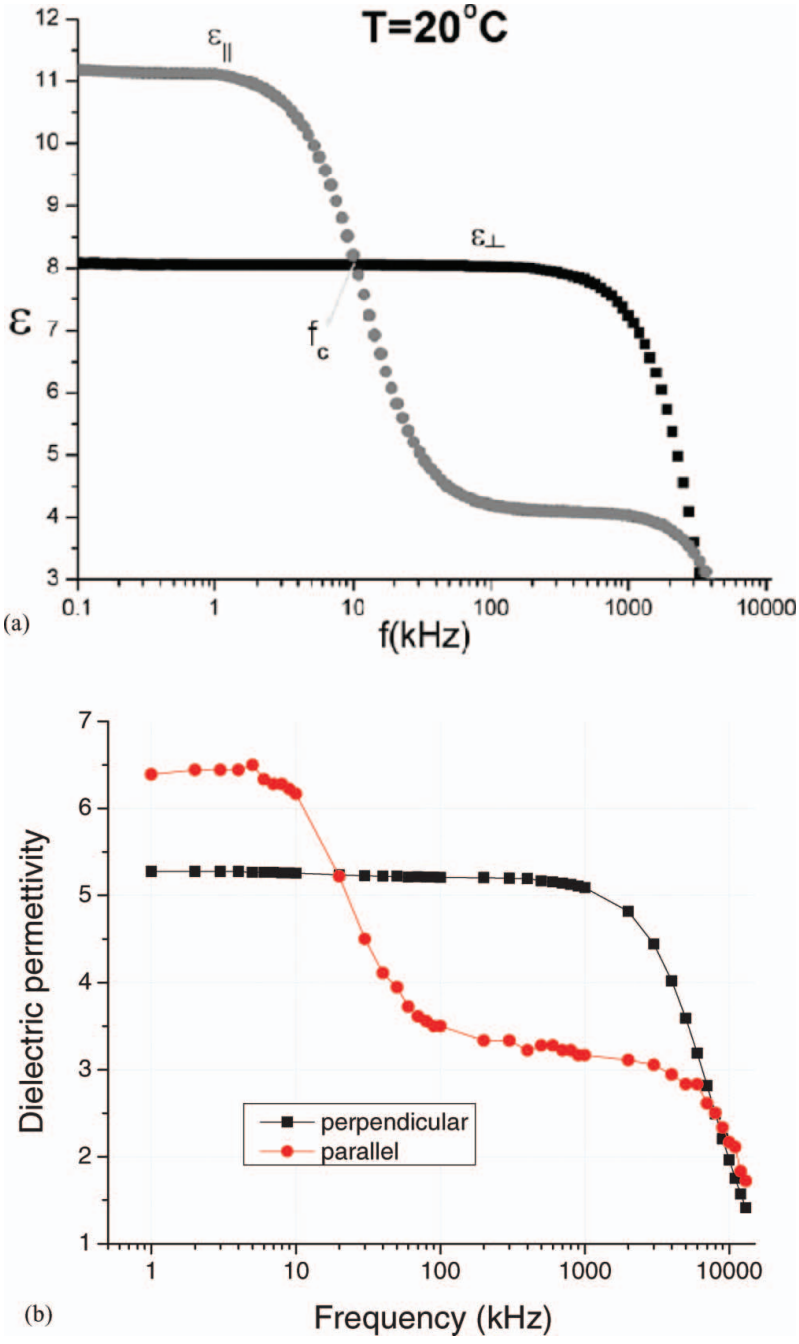

Figure 2. MLC 2048's parallel and perpendicular dielectric permittivity dependences upon the electric field frequency. (a) from Ref. [21] and (b) obtained by our approximate technique.

in water, 8–10 min. in acetone and 8–10 min. in isopropanol), then they were lifted slowly from the isopropanol and leaved in the oven to dry. Those substrates were then spin coated (500 rpm during 5 seconds, then 3000 rpm during 20 seconds) with planar alignment Polyimide layer (PI 150, from Nissan) and heated in the oven ($T = 80^{\circ}C$; during $t = 15$ minutes and then heated again at $T = 280^{\circ}C$; during $t = 60$ minutes, then slowly cooled down to room temperature). The obtained substrates were then unidirectionally rubbed to obtain planar alignment of LC mixtures. The UV sensitive adhesive NOA 65 (mixed with glass spacers, see below) was applied to seal the LC cell.

Immediately after the fabrication process was completed, some defect structures were initially observed, which then were gradually resorbed without further treatment. The application of electrical fields accelerated this uniformization process. Three cells were fabricated for the initial comparative estimations; first two cells were filled with the same mixture (Mix 33) but had different thicknesses (5 μm and 8 μm), further named, respectively cell 1 and cell 2, and the third one had small thickness (5 μm) but contained the Mix 41, further named cell 3.

Spectral studies identified the band gap positions being in the range of 1400 nm–1600 nm and 1000 nm–1200 nm, respectively, for compounds Mix 33 and Mix 41. The electrical excitation of obtained cells (AC, SIN shaped, at 1 kHz) have shown that the dielectric anisotropies of both mixtures are, in fact, positive since we were able to destroy their reflection resonances. Figure 3 demonstrates (by using polarizing microscope Zeiss) the electrical unwinding of obtained helicoidal structures by using a low frequency field (the microscope polarizers are always crossed). Thus, at the beginning, the cell is in the planar state (helicoidal structure, Fig. 3(a)), then an excitation voltage (AC, SIN shaped, 50 V RMS, 1 kHz) is applied to unwind the helix and to transfer it into homeotropic state (Fig. 3(c)). This happens through the generation of multiple transient disclinations (Fig. 3(b)). The speed of this "excitation" transition is easy to control by the applied voltage value.

Figure 4 demonstrates (by using the same polarizing microscope, in the same experimental conditions as described above) the "free-relaxation" (or natural restoring) of the cholesteric mixture when the voltage is simply switched off from the homeotropic (unwound) state, Fig. 4(a)). The various stages of this back transition may be seen in Figs 4(b)–(f). The approximate time intervals between those photos are as follows: b) is taken immediately after switching the field OFF, then c) and d) are taken with approximately 1–2 seconds of intervals, e) is taken after about a minute and f) is taken after several more minutes.

The approximate quasi thresholds of the electrical unwinding of the CLC helix for our three cells were measured to be $U_{th\,1} \approx 50$ V, $U_{th\,2} \approx 80$ V and $U_{th\,3} \approx 100$ V. Thus, the

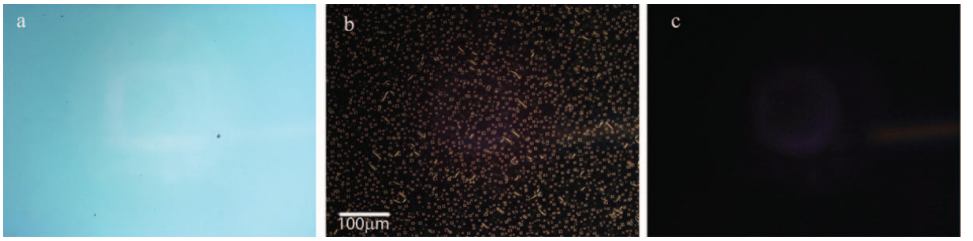

Figure 3. Polarizing microscope photohraphies of the cell (placed between crossed polarizers) taken when the voltage, applied to the cell, is switched (increased step-wise and kept constant) from planar/helicoidal to homeotropic state; a) helicoidal state, b) transient state and c) homeotropic state.

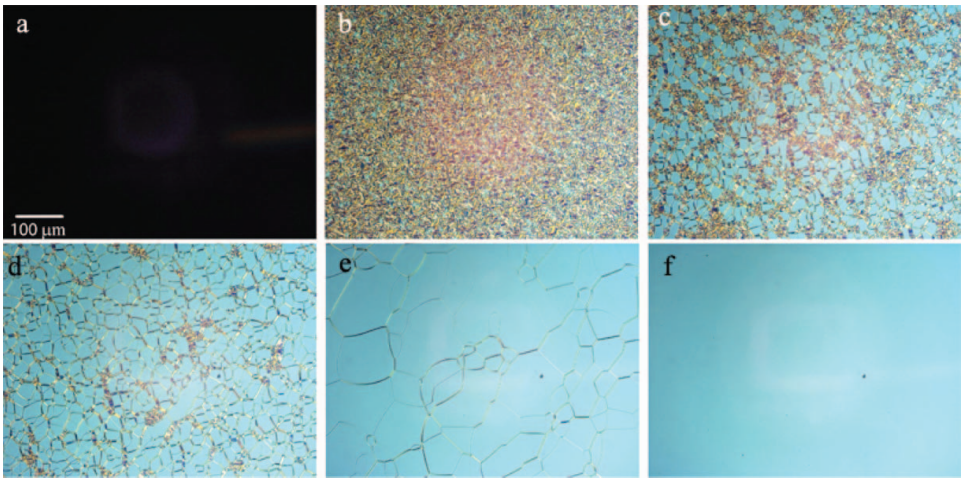

Figure 4. Polarizing microscope photohraphies of the cell (placed between crossed polarizers) taken when the cell is naturaly relaxed from the unwound homeotropic state to planar (helicoidal) state, a) homeotropic state, b)-c)-d)-e) transient states, f) planar/helicoidal state.

increase of the thickness of the cell (for the same mixture), e.g. by a factor of 1.6, increases the U_{th} by a factor of 2. In the same time, the decrease (e.g., by a factor of 1.3) of the concentration of the MLC 2048 increases the value of U_{th} by a factor of 1.6. This last effect is quite natural since the MLC2048 is responsible for the positive dielectric anisotropy at 1 kHz and, respectively, for the helix unwinding.

Time Resolved Measurements

To obtain quantitative data for the helix unwinding and restoring processes, we have built the experimental set-up described in the Fig. 5. First, a CW He–Ne laser (operating at 632.8 nm, which is out of CLC's resonance) was used as probe to observe the excitation

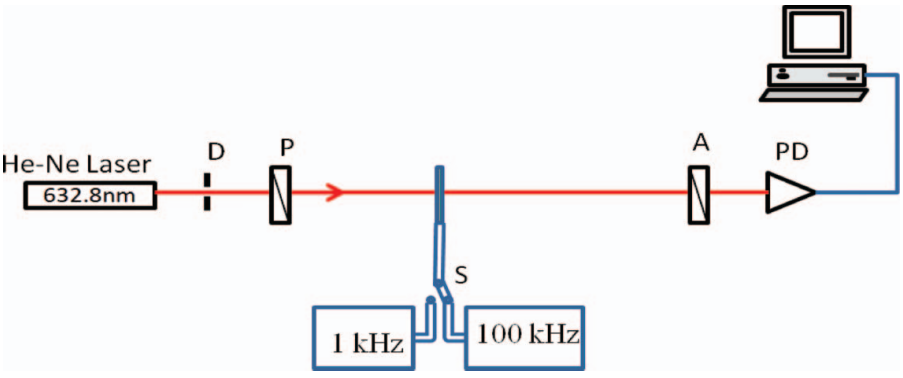

Figure 5. Schematic representation of the experimental setup used for time resolved transition measurements. D: diaphragm (1 mm), P: polarizer, A: analyzer (polymer films), PD: photodiode (at approximately 50 cm from the cell; active area diameter of the detector is d ≈ 2 mm), "1 kHz" and "100 kHz" designate generators of voltages at those frequencies.

and relaxation processes by monitoring the effective birefringence changes of the cell. Namely, the cell was placed between crossed polarizers and the cell's orientational state (homeotrope - planar) was changed by changing the voltage and frequency of the electrical signal applied to the ITOs. The probe, passing through the polarimetric system (the cell is placed between crossed polarizers), was detected by a photodiode PD, connected to the computer (taking the data at every 50 milliseconds).

The experimental procedure, used for our studies, was the following. The cell had helicoidal (planar) alignment in the ground state (U = 0 V, see Fig. 6(a)). Then, a nearly above-threshold voltage (as mentioned above, different, for different thicknesses and different mixtures) was applied to the cell (at $t \approx 3$ sec) with 1 kHz frequency (AC, SIN shaped). The transition of the cell was then monitored (approximately during 2 sec) up to the stabilization of the transmitted signal. Then, at $t \approx 5$ sec, the frequency of the electrical signal was switched from 1 kHz to 100 kHz. This was done by using a homemade mechanical switch between two generators (with a typical switching time significantly less than 0.1 sec). The restoring of the initial state was then monitored, again, up to the stabilization of the signal.

The obtained experimental results are qualitatively similar for all three cells and may be resumed as follows. The transmission of the probe is initially high (defined by the effective birefringence of the cell in the ground state), Fig. 6. Then this transmission drops drastically with the application of the voltage at 1 kHz. This transition is rather monotone since it is driven by the "positive" electric torque, the local director being "attracted" by the electric field. The simple switch-off of the voltage results into a very slow free-relaxation process (curve with U = 0 V). The natural recovery of the cholesteric helix is faster for thinner cell of the same mixture. However, this recovery is very slow for the thin cell containing smaller quantity of the CB15 compound, probably because of the smaller elastic constants of the MLC2048 compared to those of CB15 (unknown for the moment).

The recovery of transmission is accelerated if the voltage is maintained, but the frequency of the electric field is changed to 100 kHz. The applied voltage always accelerates the transmission restoring process for all three different cells. This acceleration is more pronounced if the voltage (at 100 kHz) is higher. It is worth to note that the recovery process (particularly for high voltages) is non monotonic since it is based on the "negative" dielectric torque, the local director being "repulsed" from the electric field. This repulsion initially happens in various directions, later being counter-balanced by the influence of surface rubbing that is favoring the monocrystal planar alignment. The repulsion process is obviously stronger and faster for stronger field values, which is responsible for the non monotone peak. Another feature that is common for all three cells: there's a certain saturation voltage value (at 100 kHz) after which, the farther increase of the voltage doesn't change noticeably the restoration process. This value corresponds to electric field strength $\sim$8 V/μm. Figure 7 shows the recovery processes of three cells under the action of different voltages, but the same electric field strength (2 V/μm).

Although the recovery process isn't the fastest in the case of the cell 1, we continued our investigations with that cell. The reason of this choice is that the cell 1 has the lowest helix unwinding voltage ($U_{th\,1} \approx 50$ V). To quantify the restoring speed in a very preliminary and approximate way, we fit our experimental curves (Fig. 6) with an exponential function $T = A - B^{*}exp(-t/\tau)$, where T is light's transmission across the polarimetric system, A and B are constants defining the maximum and minimum values of transmission, t is the time and τ is the restoring characteristic time. We present, in the Table 1, the fitting results, which show qualitatively the change of the recovery process under the action of the electric field, oscillating at 100 kHz frequency.

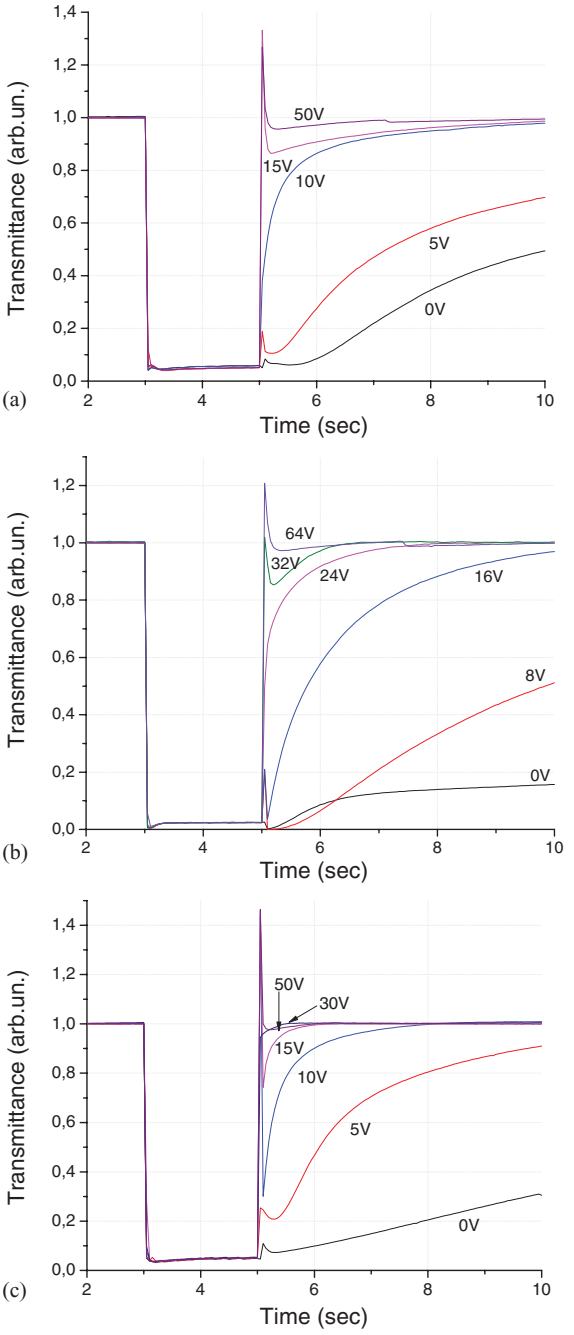

Figure 6. Variations of the polarimetric system's (CLC cell is placed between crossed polarizers) transmittance during the excitation and relaxation processes for a) Cell 1 b) Cell 2 and c) Cell 3. The high transmission corresponds to the blue state at Fig. 3(a), the low transmission to the dark state at Fig. 3(c). There was no voltage applied up to ∼3 sec, then the helix unwinding voltage (U = 50 V RMS, AC, SIN shaped at 1 kHz) was applied from ∼3 sec to ∼5 sec and finally, the restoring voltage (AC, SIN shaped at 100 kHz) was applied starting from ∼5 sec up to ∼10 sec (voltage RMS values are shown next to curves).

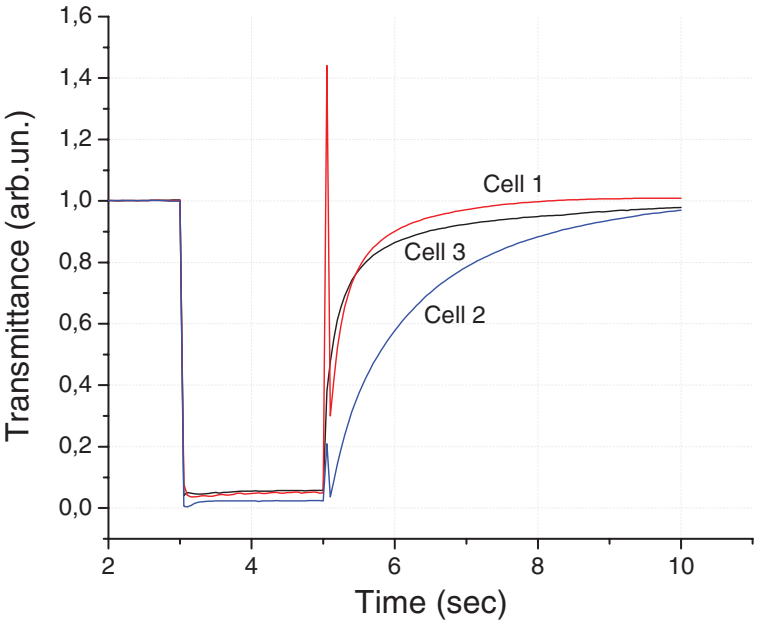

Figure 7. Variations of the polarimetric system's (the CLC cell 1 placed between crossed polarizers) transmittance during the excitation and relaxation processes (high transmission : blue state at Fig. 3(a); low transmission : dark state at Fig. 3(c); then scattering and reconstruction). There was no voltage applied up to ∼3 sec, then the helix unwinding voltage (U = 50 V (cell 1), U = 80 V (cell 2), U = 100 V (cell 3) RMS, AC, SIN shaped at 1 kHz) was applied from ∼3 sec to ∼5 sec as excitation voltage and finally, the restoring voltage (AC, SIN shaped at 100 kHz) was applied from ∼5 sec up to ∼10 sec. All three cells are under the action of the same relaxation electric field strength (2 V/μm: U = 10 V (cell 1), U = 16 V (cell 2) and U = 10 V (cell 3)).

To observe directly the helix restoration process (instead of monitoring the effective birefringence of the cell), we used another experimental setup where a fiber diode laser, operating at 1481 nm, was used to be in the resonant band of the CLC mixture (see Fig. 8). The laser beam was collimated by a microlens, then passed through the diaphragm (D), the polarizer (P) and the quarter wave plate ($\lambda/4$). Thus the probe beam become circularly polarized (by rotating the quarter—wave plate's axis to 90°, the circularity sign was changed). We measured (at every 0.1 sec) the reflected beam from the CLC cell by using the photodetector (PD) connected to a PC. The cell was very slightly tilted so that the incidence angle was approximately 0.75°.

The experimental procedure was similar to the first experiment, where the applied (to the CLC cell's ITOs) voltage's frequency was changed and the photodetector's signal changes were monitored during the excitation and relaxation processes. The cell had planar

Table 1. Fitting results

Restoring voltage (RMS Volts)	0	5	10	15
Restoring characteristic time τ (sec.)	>10	2	0.35	< 0.2

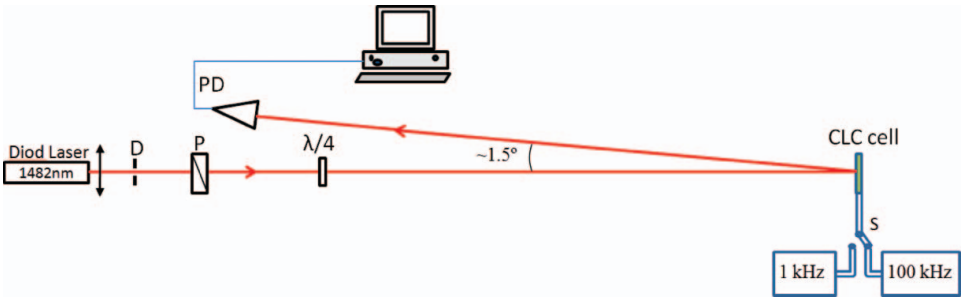

Figure 8. Schematic representation of the experimental setup used for observing the helix restoration process. D: diaphragm (∼1 mm of diameter), P: polarizer, PD: photodiode, 1 kHz and 100 kHz: voltage sources at different frequencies.

(helicoidal) alignment in the ground state (U = 0 V), see Fig. 9(a)). Then, a nearly above-threshold voltage (U = 50 V) was applied to the cell (at $t \approx 3.4$ sec) with 1 kHz frequency (AC, SIN shaped). The transition of the cell was monitored (approximately during 6.6 sec) up to the stabilization of the signal. Then, at $t \approx 10$ sec, the frequency of the electrical signal was switched (by using a homemade mechanical switch with a typical switching time significantly less than 0.1 sec) from 1 kHz to 100 kHz and the restoring of the initial state was monitored, again up to the stabilization of the signal.

Let's emphasize again the three differences from the first experiment : the probe wavelength is inside the cholesteric mixture's bandgap, the probe beam is polarized circularly and we monitor the reflected (from the CLC cell) beam.

Results

First right and then left circularly polarized probe beams were used. We see, in the Fig. 9(a)), that the application (at $t \approx 3.4$ sec) of the unwinding electrical field (oscillating at 1 kHz) decreases the reflected beam's power abruptly. When we switch off the applied voltage, the reflection starts to increase but very slowly. Other curves (in the Fig. 9(a)) show that the application and the increase of restoring voltage (at frequency of 100 kHz) accelerates the recovery process (curves U = 10 V, U = 20 V and U = 30 V). If, in the case of U = 0 V, the recovery process is much longer than 15 seconds, in the case of U = 30 V (∼6 V/μm), the reflection is restored in approximately 7 seconds. Figure 9(b) presents the results of a similar measurement but prformed for the opposite circular polarization (probe is left circularly polarized and the helix is right–handed). We see, that the probe beam reflection is the same (at least the same order of magnitude) after stabilisation in all three time intervals: 0–3.4 sec (planar/helicoidal), 3.4–10 sec (homeotrope) and from 10 sec to the end (restoring the planar/helicoidal structure).

To obtain some approximate characterisation data for the acceleration of the forced restoring, we used a similar fit with the equation $T = A - B^{*}exp(-t/\tau)$. From each fitting we have taken a value of τ (the time during which the transmission changes e times). Fitting has been done for the right (resonant) circularly polarized light, Fig. 9(a). Figure 10 shows the results of the fitting. It is clear that the application of the restoring electric field makes the relaxation process faster. The electric field U = 30 V (oscilating at 100 kHz of frequency), makes the process faster by a facter of 20 compared with the case of free relaxation.

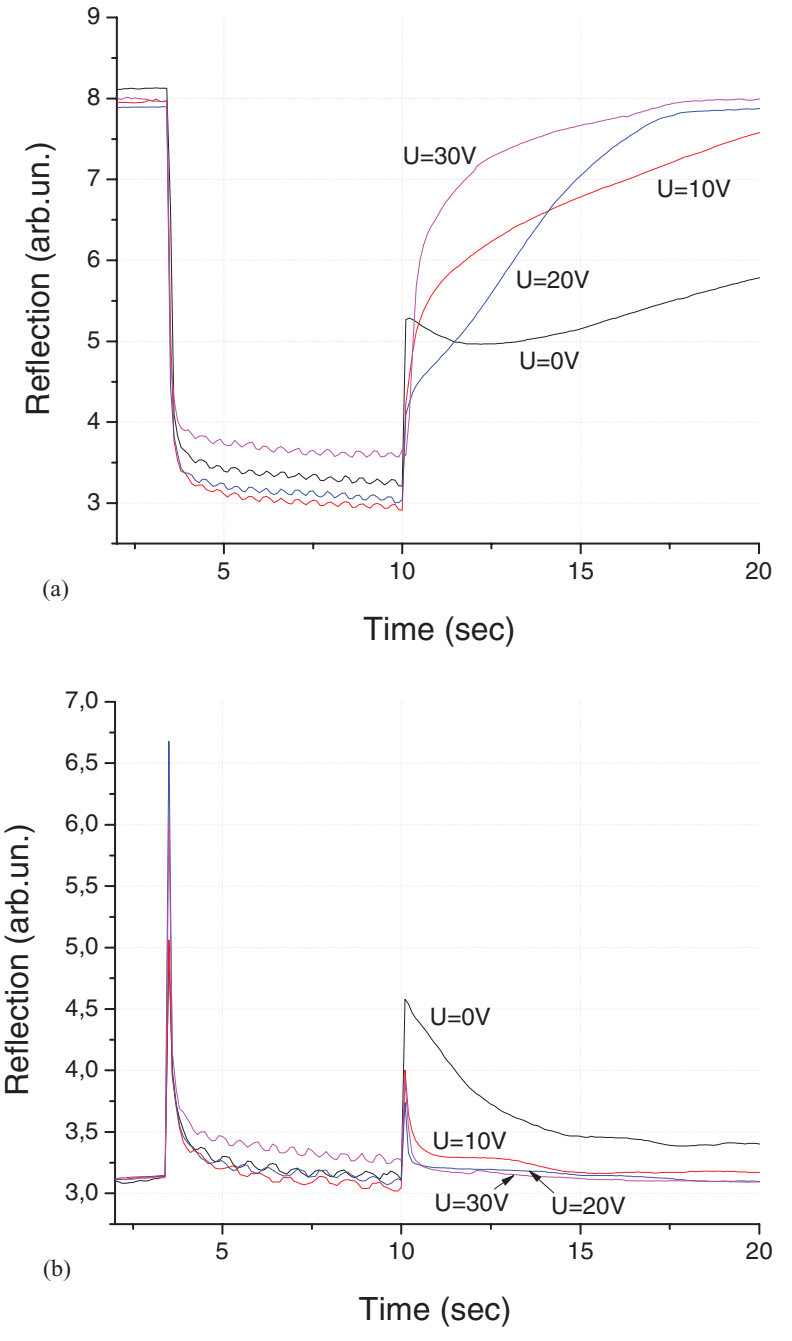

Figure 9. (a) Right and (b) Left circularly polarized ligth's reflectance (from the right handed CLC cell 1) variations in time during the excitation (helix unwinding) and relaxation (helix restoring) processes. There is no voltage applied up to ∼3.4 sec. The helix unwinding voltage (U = 50 V RMS, AC, SIN shaped, at 1 kHz) was applied from ∼3.4 to ∼10 sec. The restoring voltage (AC, SIN shaped, at 100 kHz) was applied from ∼10 sec up to 20 sec (relaxation voltage RMS values are shown next to curves).

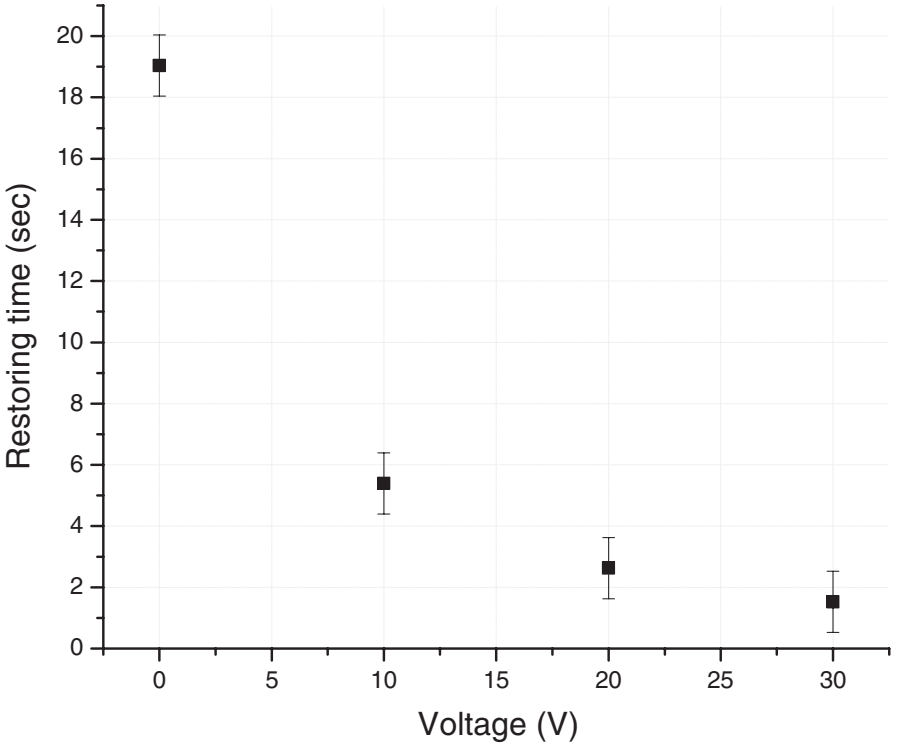

Figure 10. The helix restoring characteristic time's dependence upon the applied voltage at 100 kHz for the 5 μm thick cell filled with the Mix33.

Summary and Conclusions

We have shown that the helix restoring process of a cholesteric mixture may be accelerated (by approximately an order of magnitude) by the use of high frequency electrical field where the dielectric anisotropy of the mixture is negative. Thus, the applied field helps to restore and to stabilize the helix. We have also studied the process of electrical unwinding to show that the process takes place through the simultaneous generation of multiple defects. In contrast, the free relaxation process of the helix restoring involves the formation of long disclination walls and their merge.

Despite the good acceleration obtained, the restoring process is still not fast enough, e.g., for telecommunication or imaging applications. Further optimization of composition, thicknesses and driving voltages and frequencies must be done before a practical use of the composition.

Acknowledgment

We thank the financial support of Canadian Institute for Photonic Innovations (CIPI), Fonds Québécois de la Recherche sur la Nature et les Technologies (FQRNT) and Natural Sciences and Engineering Research Council of Canada (NSERC).

References

[1] Yeh, P., & Gu, C. (1999). *Optics of Liquid Crystal Displays*, Wiley.

[2] Blinov, L. M., & Chigrinov, V. G. (1994). *Electrooptic Effects in Liquid Crystal Materials*, Springer.

[3] de Gennes, P. G., and Prost, J. (1995). *The Physics of Liquid Crystals*, Oxford University Press, 2nd Edition.

[4] Belyakov, V. A., Dmitrienko, V. E., & Orlov, V. P. (1979). Optics of cholesteric liquid crystals. *Soviet Physics Uspekhi*, *22*(2), (*Sov. Phys. Usp. 22*(64)).

[5] Finkelmann, H., Kim, S. T., Muæoz, A., Palffy-Muhoray, P., & Taheri, B. (2001). Tunable mirrorless lasing in cholesteric liquid crystalline elastomers. *Adv. Mater.*, *13*(14), 1069–1072.

[6] Chilaya, G., Chanishvili, A., Petriashvili, G., Barberi, R., Bartolino, R., Cipparrone, G., Mazzulla, A., & Shibaev, P. V. (2007). Reversible tuning of lasing in cholesteric liquid crystals controlled by light-emitting diodes. *Adv. Mater.*, *19*, 565–568.

[7] Huang, Y., Zhou, Y., Doyle, C., & Wu, S.-T. (2006). Tuning the photonic band gap in cholesteric liquid crystals by temperature-dependent dopant solubility. *Optics Express*, *14*(3), 1236–1242.

[8] Yip, W. C., & Kwok, H. S. (2001). Helix unwinding of doped cholesteric liquid crystals. *Applied Physics Letters*, *78*(4), 425–427.

[9] Belyakov, V. A. (2002). Untwisting of the helical structure in a plane layer of chiral liquid crystal. *JETP Letters*, *76*(2), 88–92.

[10] Bailey, C. A., Tondiglia, V. P., Natarajan, L. V., Duning, M. M., Bricker, R. L., Sutherland, R. L., White, T. J., Durstock, M. F., & Bunning, T. J. (2010). Electromechanical tuning of cholesteric liquid crystals. *Journal of Applied Physics*, *107*, 013105.

[11] Natarajan, L. V., Wofford, J. M., Tondiglia, V. P., Sutherland, R. L., Koerner, H., Vaia, R. A., & Bunning, T. J. (2008). Electro-thermal tuning in a negative dielectric cholesteric liquid crystal material. *Journal of Applied Physics*, *103*, 093107.

[12] Uladzimir A. Hrozhyk, Svetlana V. Serak, Nelson V. Tabiryan, Timothy J. White, & Timothy J. Bunning. (2011). Nonlinear optical properties of fast, photoswitchable cholesteric liquid crystal bandgaps. *Optical Materials Express*, *1*(5), 943–952.

[13] Allahverdyan, K., & Galstian, T. (2011). Electrooptic jumps in natural helicoidal photonic bandgap structures. *Optics Express*, *19*(5), 4611–4617.

[14] Broer, D. J., Lub, J., & Mol, G. N. (30 November 1995). Wide-band reflective polarizers from cholesteric polymer networks with a pitch gradient. *Nature*, *378*, 467–469.

[15] Mitov, M., Nouvet, E., & Dessaud, N. (2004). Polymer-stabilized cholesteric liquid crystals as switchable photonic broad bandgaps. *Eur. Phys. J. E*, *15*, 413–419.

[16] Lu, S.-Y., & Chien, L.-C. (2007). A polymer-stabilized single-layer color cholesteric liquid crystal display with anisotropic reflection. *Applied Physics Letters*, *91*, 131119.

[17] Relaix, S., & Mitov, M. (2008). Polymer stabilised cholesteric liquid crystals with a double helical handedness: influence of an ultraviolet light absorber on the characteristics of the circularly polarised reflection band. *Liq. Cryst.*, *35*, 1037.

[18] Gonzague Agez, & Michel Mitov. (2011). Cholesteric liquid crystalline materials with a dual circularly polarized light reflection band fixed at room temperature. *J. Phys. Chem. B*, *115*, 6421.

[19] Yu-Cheng Hsiao, Chen-Yu Tang, & Wei Lee. (2011). Fast-switching bistable cholesteric intensity modulator. *Opt. Express*, *19*, 9744–9749.

[20] Jewell, S. A., & Sambles, J. R. (2007). Measurement of azimuthal backflow in dual-frequency chiral HAN cell. *Mol. Cryst. Liq. Cryst.*, *477*, 551.

[21] Jewell, S. A., & Sambles, J. R. (2006). Dynamc response of a dual-frequency chiral hybrid aligned nematic liquid-crystal cell. *Physical Review E*, *73*, 011706.

[22] Huang, C. Y., & Khuang-Yu Fu. (2003). Bistable transflective cholesteric ligth shutters. *Optics Express*, *11*, 560.

[23] Xu, M., & Yang, D. K. (1999). Electrooptical properties of dual-frequency cholesteric liquid crystal reflective display and drive scheme. *Jpn. J. of Appl. Phys. Part 1*, *38*, 6827.

[24] Xu, M., & Yang, D. K. (1997). Dual frequency cholesteric ligth shutters. *Appl. Phys. Lett.*, *70*, 720.

[25] Wenbo Li, Hongxue Zhang, Liping Wang, Canbin Ouyang, Xiaokang Ding, Hui Cao, & Huai Yang. (2007). Effect of a chiral dopant on the electro-optical properties of polymer-dispersed liquid-crystal films. *Journal of Applied Polymer Science* DOI 10.1002/app.

[26] EMD Chemicals Inc., Hawthorne, New York, 10532-2156, Tel: 914-592-4660. http://www.emdchemicals.com.

[27] Yun-Hsing Fan, Hongwen Ren, Xiao Liang, Yi-Hsin Lin, & Shin-Tson Wu. (2004). Dual-frequency liquid crystal gels with submillisecond response time. *Applied Physics Letters*, *85*(13), 2451.

[28] Andrii B. Golovin, Sergij V. Shiyanovskii, & Oleg D. Lavrentovich (2003). Fast switching dual-frequency liquid crystal optical retarder, driven by an amplitude and frequency modulated voltage. *SID DIGEST*, *55.2*, 1472.

[29] Ye Yin, Mingxia Gu, Andrii B. Golovin, Sergij V. Shiyanovskii, & Oleg D. Lavrentovich. (2004). Fast switching optical modulators based on dual frequency nematic cell. *Mol. Cryst. Liq. Cryst.*, *421*, 133–144.